To be submitted to ApJ

ORIGIN OF LOW- AND INTERMEDIATE-MASS STARS IN OB ASSOCIATIONS

Hsu-Tai Lee[1]

eridan@astro.ncu.edu.tw

W. P. Chen[1,2]

wchen@astro.ncu.edu.tw

ABSTRACT

We present our diagnosis of the role massive stars play in the formation of low- and intermediate-mass stars in OB associations. In the bright-rimmed and comet-shaped clouds in both the Ori OB1 and Lac OB1 associations, there is compelling evidence of low- and intermediate-mass star formation dominated by the triggering process by the massive stars in the regions. The expanding ionization fronts from the O stars appear to have compressed nearby molecular clouds which are engraved and shaped into bright-rimmed or comet-shaped clouds. Implosive pressure on the surface layers then causes a cloud to collapse and prompts subsequent formation of stars, including low- and intermediate-mass stars. The triggering process may propagate through one cloud after another, and the majority of the stellar population in an entire OB association with a scale of tens of parsec may be formed in the sequence.

Subject headings: stars: formation — stars: pre-main-sequence — ISM: clouds — ISM: molecules

1. INTRODUCTION

Most O and B stars congregate to form OB associations (see Blaauw 1964 for a review), with which young low- (classical T Tauri stars, or CTTSs) and intermediate-mass (Herbig

[1]Institute of Astronomy, National Central University, Taiwan 320, R.O.C.

[2]Department of Physics, National Central University, Taiwan, 320, R.O.C.

Ae/Be stars, or HAeBe) stellar groups are also found. What is the relationship between the formation of massive stars and of low-mass stars? Does star formation in an OB association proceed in a bimodal manner for massive and for low-mass stellar groups? If so, which groups, low- or high-mass stars, would form first? Even a single O star has a profound influence on the surrounding molecular clouds. On the one hand, the radiation and energetic wind from the O star could evaporate nearby clouds and henceforth terminate the star-forming processes. On the other hand the O star may provide "just the touch" to prompt the collapse of the molecular cloud which otherwise may not contract spontaneously. Do massive stars play a decisively destructive or promotive role in sustaining the star formation in a molecular cloud? Herbig (1962) suggests that low- and intermediate-mass stars form first, but soon after O stars appear the cloud is disrupted to hinder any further star formation. Alternatively, Elmegreen & Lada (1977) and Lada (1987) propose that low-mass stars form first out of cloud fragments and are distributed throughout the entire molecular cloud. Once the O stars form, their expanding ionization fronts (I-fronts) play a constructive role to incite a sequence of star-forming actives in neighboring molecular clouds.

The Scorpius-Centaurus association as a consequence of triggered star formation is suggested by de Geus et al. (1989). In their scenario, the Upper-Centaurus Lupus subgroup was formed first in the middle of the molecular cloud complex, and then prompted the star formation on both sides to become eventually the Upper-Scorpius and Lower-Centaurus Crux associations. Preibisch & Zinnecker (1999) propose a similar mechanism, but with a series of supernova explosions as the triggering sources.

In the Orion star-forming region, we have found (Lee et al. 2005, hereafter Paper I) concrete evidence of triggered star formation in the bright-rimmed clouds (BRCs) in the vicinity of O stars. These BRCs are considered to be remnant molecular cloud(s) photoionized by a nearby luminous star. Observations in BRCs, B 35, B 30, IC 2118, LDN 1616, LDN 1634, and Ori East indicate that only BRCs associated with strong *IRAS* 100 μm emission (tracer of high density) and Hα emission (tracer of ionization front) show signs of ongoing star formation. Furthermore, CTTSs are only seen between the O stars and the BRCs, with those closer to the BRCs being progressively younger, and there are no CTTS leading the I-fronts, i.e., within the molecular clouds. All these lend support to the scenario of sequential star formation by the radiation-driven implosion (RDI) mechanism (Bertoldi 1989; Bertoldi & McKee 1990) for which the I-fronts from an O star or a group of OB stars compress a nearby cloud until the density of the compressed region exceeds the critical value, thereby inducing the cloud to collapse to form stars (Paper I).

In this paper we extend the discussion to the Lac OB1 association and include intermediate-mass young stars in our sample. The Lac OB1 association, with a distance of $\sim$360 pc (de

Zeeuw et al. 1999), is one of the nearest OB associations. Blaauw (1958) divides Lac OB1 into 2 subgroups, "a" and "b", based on stellar proper motions and radial velocities. The Lac OB1 occupies the sky region 90°< l < 110°, -5°< b < -25°(de Zeeuw et al. 1999) in which Lac OB1b centers at (l, b)=(97°.0, -15°.5) with a radius ∼5°with the remaining for Lac OB1a. The Lac OB1b is about 358 pc away from us (de Zeeuw et al. 1999) and harbors the only O star (O9 V), 10 Lac, in the Lac OB1 association.

We describe in §2 the archive data and our spectroscopic and imaging observations used for this study. In addition to the Lac OB1 sources, some of the stars in Ori OB1 previously identified to be young star candidates in Paper I have been confirmed by spectroscopy. They are also presented here. In §3 we present evidence of triggered star formation in the BRCs in the Lac OB1 association. In §4 we discuss the star formation history in an OB association. The conclusions are summarized in §5.

2. DATA AND OBSERVATIONS

2.1. ARCHIVE DATA

CTTSs are young stellar objects characterized by their infrared excess. Usually CTTSs are spatially closer to a star-forming region than weak-line T Tauri stars (WTTSs) are, which are also pre-main sequence (PMS) stars but more evolved than CTTSs in terms of clearing of circumstellar disks. The CTTSs hence trace recent star formation. In Paper I, we have developed an empirical set of criteria to utilize the 2MASS Point Source Catalog (Cutri et al. 2003) to select CTTS candidates. In this paper, we apply the same procedure (e.g., 2MASS colors, good photometric qualities, and exclusion of extended sources) and include young intermediate-mass stars, HAeBe stars (Waters & Waelkens 1998) into our sample. Different young stellar populations, WTTSs, CTTSs, and HAeBe stars occupy distinctly different regions in the 2MASS color-color diagram. HAeBe stars in general exhibit larger infrared excesses than CTTSs do. Therefore we select 2MASS point sources as HAeBe candidates with colors redder than the line defined by $(m_J - m_H) - 1.7(m_H - m_K) + 0.450 = 0$ and select CTTS candidates by the same method described in paper I, namely between the two parallel lines, $(m_J - m_H) - 1.7(m_H - m_K) + 0.0976 = 0$ and $(m_J - m_H) - 1.7(m_H - m_K) + 0.450 = 0$, and above the dereddened CTTS locus ,$(m_J - m_H) - 0.493(m_H - m_K) - 0.439 = 0$.

Table 1 shows the fields respectively in the Ori OB1 and Lac OB1 associations studied in this paper, including 7 BRCs, one comet-shaped cloud and two control regions. In addition to the 2MASS database, from which we select our CTTS and HAeBe candidates, we have also made use of survey data of the Hα emission (Finkbeiner 2003; Gaustad et al. 2001),

$E(B-V)$ reddening (Schlegel et al. 1998), *IRAS* 100 μm, and CO (Dame et al. 2001) emission to trace, respectively, the distribution of ionization fronts, cloud extinction, IR radiation, and molecular clouds with respect to the spatial distribution of our young star sample.

2.2. SPECTROSCOPIC OBSERVATIONS

Spectra of bright CTTS and HAeBe candidates were taken at the Beijing Astronomical Observatory (BAO) and at the Kitt Peak National Observatory (KPNO). At the BAO, low-dispersion spectra with a dispersion of 200 Å mm^{-1}, 4.8 Å $pixel^{-1}$, were taken with the 2.16 m optical telescope during 2003 October 31 to November 3, and during 2004 September 5–6. An OMR (Optomechanics Research, Inc.) spectrograph was used with a Tektronix 1024×1024 CCD detector covering 4000-9000 Å. These spectra were used to confirm the young stellar nature (e.g., with H-alpha and other characteristic emission lines) of the PMS candidates selected on the basis of the 2MASS colors.

Medium-dispersion spectra were taken for a selected set of the sample stars with the KPNO 2.1 m telescope during 2004 January 2-5. The GoldCamera spectrometer, with a Ford 3Kx1K CCD with 15 μm pixels, was used with the grating #26new, which gives a dispersion of 1.24 Å $pixel^{-1}$. These medium-dispersion spectra allowed us to identify the lithium absorption at 6708 Å, the signature of a low-mass PMS star.

All the spectroscopic data were processed with standard NOAO/IRAF packages. After the bias and flat-fielding correction, the IRAF package KPNOSLIT was used to extract, and to calibrate the wavelength and flux of each spectrum. To check the legitimacy of our selection criteria, we also observed two control fields in addition to star-forming clouds. All the fields included in this study are summarized in Table 1.

2.3. IMAGING OBSERVATIONS

The BRCs were imaged in 2004 November 3–8 using the 1 m telescope at Lulin Observatory in Taiwan (Table 2). A PI 1300B (Roper Scientific) CCD camera was used, which has 1340×1300 pixels, each of 20 μm squared, yielding a $\sim 11'$ field of view. The Hα (λ_c=6563 Å, $\Delta\lambda$(FWHM)=30 Å) images were taken for all BRCs. In addition, LBN 437 was observed with a [S II] (λ_c= 6724 Å, $\Delta\lambda$(FWHM)=80 Å) filter. For every target field tens of images were taken, each with an exposure time 120 to 300 s. The images were processed with standard procedures of bias, dark and flat-fielding corrections.

2.4. OBSERVATIONAL RESULTS

Table 3, 4, and 5 list respectively the CTTSs (plus some CTTS candidates), HAeBe stars, and non-PMS sources identified with our spectroscopic observations. Some of the CTTSs listed in Table 3 do not show lithium absorption, but exhibit other CTTS characteristics, e.g. Hα, Ca II, and/or forbidden [O I] and [S II] emission line(s) in their spectra. Since most of these spectra show veiling, their Li absorption line could have been veiled by their continuum radiation. We hence include them in the CTTS sample (Table 3) even though the Li line is not readily discerned. No PMS stars have been found in any of the two control fields; most of the sources there are either carbon stars or M giants.

Figure 1 and Figure 2 show respectively the overview of the Trapezium and λ Ori regions in Orion. The PMS stars listed in Table 3 (CTTSs) and Table 4 (HAeBe stars) are marked. The boxes are the regions where we present the Hα images in Fig. 3. It is clear that the BRCs are outlined by the Hα emission (I-fronts). Some PMS stars are closely associated with the I-front structure. These stars are born by triggered star formation (Paper I), and the Trapezium or λ Ori is responsible for the formation of these stars. In B 30 and B 35, photoevaporative flows (Hester et al. 1996) stream out of the surfaces of BRCs, an outcome of interaction between the O star and the molecular clouds.

Figure 4 displays the *IRAS* 100 μm, Hα and CO images of the Lac OB1 association. The PMS stars in Table 3 and Table 4 are again marked. The box indicates the region of LBN 437 in Figure 5. LBN 437 is a comet-shaped BRC (Olano et al. 1994). The HAeBe star, star 53 (V375 Lac), associated with this cloud is believed to be the exciting source of the parsec-scale HH outflow HH 398 (McGroarty et al. 2004) (see Figure 5).

3. TRIGGERED STAR FORMATION IN OB ASSOCIATIONS

A triggered star formation process has several imprints which can be observationally diagnosed: (1) The remnant cloud is extended toward, or pointing to, the massive stars. (2) The young stellar groupings in the region are roughly lined up between the remnant cloud and the luminous star, (3) Stars closer to the cloud, formed later in the sequence, are younger in age, with the youngest stars at the interacting region (i.e., bright rims of the cloud), and (4) There are no young stars within the BRC. In particular, items (3) to (4) are noticeably in contrast to the case of spontaneous star formation which conceivably would not leave such distinguishing sequential and positional signposts.

In Ori OB1, several BRCs, namely B 30, B 35, Ori East, IC 2118, LDN 1616, and LDN 1634, evince star formation triggered by nearby massive stars. Each of these BRCs is as-

sociated with strong *IRAS* 100 μm emission (Paper I), and clearly traced by H_α emission (Fig. 3). Evidence of triggered star formation by O stars and/or by superbubbles is also presented by Alcalá et al. (2004) and Stanke et al. (2002) in LDN 1616 and by Kun et al. (2001) in IC 2118.

In what follows, we present a similar study of the BRCs in Lac OB1. Combined with our previous results in Ori OB1, this reinforces the links among massive stars, BRCs, and the formation of low-mass stars. Furthermore, our young star sample now has expanded to include intermediate-mass young stars to render a more comprehensive understanding on the origin of stellar masses in an OB association.

3.1. STAR-FORMING ACTIVITIES IN LAC OB1

We present our studies of the only two regions with current star-forming activities in the Lac OB1 association, LBN 437, a BRC, and GAL 110-13, a comet-shaped cloud respectively.

3.1.1. LBN 437

LBN 437 is at the edge of an elongated molecular cloud (Olano et al. 1994) and on the border of the H II region S126, excited by the nearby O star, 10 Lac. There is a small stellar group (Fig. 6) located between 10 Lac and LBN 437, and containing 5 CTTSs (stars 35–38 in Table 3, and another CTTS candidate 2MASS J22354224+3959566 which we do not have spectroscopic observation) and one HAeBe star (star 54 in Table 4). The HAeBe star is an *IRAS* source, IRAS 22343+3944. We identify IRAS 22343+3944 as the counterpart of star 54, because star 54 shows near-infrared excess and is located within the positional error of IRAS 22343+3944. Hereafter we call this 6-star system as the IRAS 22343+3944 group (Fig. 4). The size of the IRAS 22343+3944 group is about 24′, which corresponds to $\sim$ 2.5 pc at 358 pc.

Star 53 (V375 Lac) is the only young star located on the surface of LBN 437, and there is no CTTS or HAeBe candidate behind the interaction region. This is consistent with the triggered star formation diagnosis discussed above. For each molecular cloud we test if there is any PMS star located behind the I-fronts and embedded in the cloud by an estimate of the probability of stars which would have hidden from our detection limit of $J = 15$ mag from 2MASS data. We created the $E(B-V)$ map (Schlegel et al. 1998) for the cloud, and assumed the same J band luminosities for the embedded PMS stars as those for the visible PMS stars outside the cloud, the IRAS 22343+3944 group. The extinction is quite low in

the molecular cloud and the nondetection probability is about 0.014. That means there are no PMS stars embedded in the molecular cloud and the formation of V375 Lac is the latest product in the star formation sequence by 10 Lac in this cloud.

The elongated cloud associated with LDN 437 (Fig. 4) may be just the remnant molecular cloud, originally perhaps larger and extending to as far as the position of 10 Lac. When 10 Lac was born out of the giant molecular cloud, its UV photons evaporated and compressed the cloud. That would shape the cloud into a pillar and then IRAS 22343+3944 group and V375 Lac were born in the compressed side of the molecular cloud. Because V375 Lac is the exciting source of an HH outflow, it is likely younger than the IRAS 22343+3944 system. We are manifested here the consequence of sequential star formation.

3.1.2. GAL 110−13

GAL 110−13 is an isolated and elongated molecular cloud (Fig. 7) at a distance of $\sim$ 440 pc (Odenwald et al. 1992). Its head-tail or comet-like shape suggests compression by ram-pressure, perhaps as a result of a recent cloud collision (Odenwald et al. 1992). Star formation takes place in the compressed side of the cloud, i.e., CTTS star 40 (BM And) and reflection nebula vdB 158 reflected light from the B9.5V star HD 222142 (Magakian 2003). Besides HD 222142, there are two other late B-type stars in the vicinity, HD 222046 and HD 222086. All these three B stars and star 40 share common proper motions (Zacharias et al. 2004, Second U.S. Naval Observatory CCD Astrograph Catalog (UCAC2)), which do not differ significantly from those for the Lac OB1 groups (ESA 1997), as summarized in Table 6. GAL 110−13 is located near the border of the Lac OB1 association, with a distance from us not very different from that from Lac OB1 to us. Thus GAL 110−13, together with the young stars in it, is likely part of Lac OB1.

The GAL 110−13 has an elongation pointing toward 10 Lac (Fig. 4). This implies that 10 Lac or Lac OB1b is responsible for shaping the cloud. Either shock fronts from a supernova or ionization fronts from a massive star could produce the shape of the cloud and the distribution of young stars in GAL 110−13. In the supernova scenario a star in Lac OB1b, more massive than 10 Lac, exploded. Assuming the Lac OB1b and 10 Lac are at the same distances (i.e., 358 pc) from us, it would take a few hundred thousand years for the supernova shock waves, with a speed about hundreds of km s^{-1}, to propagate the 126 pc separation to arrive, compress, and prompt the formation of stars within GAL 110−13.

On the other hand, compression by ionization fronts from a massive star is less destructive than a supernova explosion. We envision a scenario in which 10 Lac — which is still

in existence now — was born at the edge of a molecular cloud, similar to that presented in Figure 4, but with the cloud more extended toward 10 Lac. After its birth, 10 Lac soon ionized the surrounding molecular cloud and exposed itself immediately to intercloud medium. Assuming all the UV photons by 10 Lac shortward of the Lyman limit were used to ionize the intercloud medium, given the density of the intercloud material $\sim$ 0.2 cm^{-3} (Spitzer 1998; Dyson & Williams 1997), the I-fronts would travel the 126 pc distance from 10 Lac to GAL 110−13 in about 2 Myr, a time scale shorter than the main sequence life time of 10 Lac, which as an O9 V star is about 3.6 Myr (Schaerer & de Koter 1997). No matter which scenario is correct, a supernova shock front or an I-front, Lac OB1b is likely responsible for the creation of the GAL 110−13 cloud and the associated stellar group.

Odenwald et al. (1992) derive a 30% star formation efficiency for GAL 110−13. This is much higher than that of a few percent typically in star-forming regions (White et al. 1995). The extinction is low in GAL 110−13, A_J less than 0.48 mag, as estimated from its $E(B-V)$ values (Schlegel et al. 1998), so the cloud is insufficient to hide any embedded young stars similar to star 40 from our detection. As in the case in Ori OB1 (Paper I), the BRCs in Lac OB1 also tend to have relatively low dust extinction. Such a low density condition is unfavorable for spontaneous cloud collapse. Star formation however may take place efficiently at the interaction layer (the bright rim) of a molecular cloud, from which a stellar group could form, as witnessed in the IRAS 22343+3944 and GAL 110−13 groups.

4. STAR FORMATION HISTORY IN OB ASSOCIATIONS

Blaauw (1964) derives the age for Lac OB1a and Lac OB1b to be 16 and 12 Myr, respectively. Both these ages are too old to be consistent with the existence of 10 Lac (age about 3.6 Myr) and the CTTSs (typical ages of a few Myr) in the region. Lac OB1a and Lac OB1b could not have formed at the same place and at the same time because, with a typical velocity dispersion of a few kilometers per second for an OB association (de Zeeuw et al. 1999), the two subgroups could not traverse the distance of 30–80 pc now between them. We propose that both Lac OB1a and Lac OB1b are no more than a few Myr old, and Lac OB1a is younger than Lac OB1b. Figure 8 shows the color-magnitude diagrams, reconstructed from de Zeeuw et al. (1999), for the two subgroups, in which the stars in Lac OB1b are seen to form a clear main sequence, whereas those in the subgroup Lac OB1a are much scattered to the right of the sequence. That implies that some stars in Lac OB1a are still in the PMS phase, and therefore that Lac OB1a is younger than Lac OB1b. It could be that Lac OB1b was formed first and subsequently initiated the formation of stars in Lac OB1a.

HAeBe stars seem to distribute spatially within a BRC differently from CTTSs do, in

the sense that CTTSs are located near the surfaces of BRCs, whereas HAeBe stars appear to reside preferentially inside BRCs, e.g., stars 45 in B 30 and star 53 in LBN 437. This result may probably reflect star formation environment, e.g. density, can affect the masses of new born stars.

In both Ori OB1 and Lac OB1, we see consistent evidence of triggered star formation. The UV photons from an O star create expanding I-fronts which evaporate and compress nearby molecular clouds, thereby shaping the clouds into BRCs or comet-shaped clouds. Next-generation stars could be formed, perhaps in groups, out of the compressed material with high star formation efficiencies. The newly formed stars would line up, in an age and formation sequence, between the massive star and the molecular clouds. In our sample (Table 4) stars as massive as late Herbig Be types could form in this process. These stars will reach the main sequence with even earlier spectral types. Triggered star formation may produce therefore not only low-mass stars, but also intermediate-mass stars. The process hence may be propagating though a giant molecular cloud, and an entire OB association on a scale of tens of parsec could be brought about (Figure 9).

Elmegreen & Lada (1977) propose different formation mechanisms for massive stars and for low-mass stars. In their scenario massive stars form in the shocked cloud layer by triggering, and low-mass stars form spontaneously throughout the cloud. Our observations in both Ori OB1 and Lac OB1 do not show such separate spatial distributions for low-mass and massive stars. At the BRC stage, it appears that low-mass stars are seen at the shocked layer and more massive stars form in the inner and denser parts of a cloud. As the I-fronts progress, eventually the remnant cloud is dispersed, and stars of different masses would remain in the same volume.

5. CONCLUSIONS

We select CTTSs and HAeBe stars based on 2MASS colors in Ori OB1 and Lac OB1 associations. These PMS stars are utilized to trace recent star-forming activities. This paper concentrates on star formation in one comet-shaped cloud, GAL 110−13 and 7 BRCs, B 30, B 35, IC 2118, LDN 1616, LDN 1634, Ori East, and LBN 437.

The spatial distributions of CTTSs and of HAeBe stars in an OB association appear to be different. These young stars line up between massive stars and comet-shaped clouds or BRCs, with the youngest stars found near the cloud surfaces. No PMS stars exist far behind the I-front. This result implies that triggered star formation dominates the birth of low- and intermediate-mass stars in the peripheral regions of an OB association. We

propose the scenario that O stars are formed in a giant molecular cloud first, and their Lyman continuum photons create expanding I-fronts which evaporate and compress nearby clouds to form BRCs or comet-shaped clouds, thereby inducing star formation. It is possible that an OB association on a scale of tens of parsec could be formed by this kind of sequence of triggered star formation.

We want to thank specially Richard F. Green, Director of KPNO, who kindly provided us director's discretionary time to accomplish this work. We thank the staff at the Beijing Astronomical Observatory for their assistance during our observing runs. This research makes use of data products from the Two Micron All Sky Survey, which is a joint project of the University of Massachusetts and the Infrared Processing and Analysis Center/California Institute of Technology, funded by the National Aeronautics and Space Administration and the National Science Foundation (NSF). We also use the Southern H-Alpha Sky Survey Atlas (SHASSA), supported by the NSF. We acknowledge the financial support of the grants NSC92-2112-M-008-047 of the National Science Council, and 92-N-FA01-1-4-5 of the Ministry of Education of Taiwan.

REFERENCES

Alcalá, J. M., Wachter, S., Covino, E., Sterzik, M. F., Durisen, R. H., Freyberg, M. J., Hoard, D. W., & Cooksey, K. 2004, A&A, 416, 677

Bertoldi, F. 1989, ApJ, 346, 735

Bertoldi, F. & McKee, C. F. 1990, ApJ, 354, 529

Blaauw, A. 1958, AJ, 63, 186

Blaauw, A. 1964, ARA&A, 2, 213

Cutri, R. M., et al. 2003, 2MASS All Sky Catalog of Point Sources (Pasadena:IPAC)

Dame, T. M., Hartmann, D., & Thaddeus, P. 2001, ApJ, 547, 792

de Geus, E. J., de Zeeuw, P. T., & Lub, J. 1989, A&A, 216, 44

de Zeeuw, P. T., Hoogerwerf, R., de Bruijne, J. H. J., Brown, A. G. A., & Blaauw, A. 1999, AJ, 117, 354

Dyson, J. E., & Williams, D. A. 1997, The Physics of the Interstellar Medium (2nd ed.; Bristol: Institute of Physics Publishing)

Elmegreen, B. G. & Lada, C. J. 1977, ApJ, 214, 725

ESA. 1997, The Hipparcos and Tycho Catalogs, 1997, ESA SP-1200

Finkbeiner, D. P. 2003, ApJS, 146, 407

Gaustad, J. E., McCullough, P. R., Rosing, W., & Van Buren, D. 2001, PASP, 113, 1326

Herbig, G. H. 1962, ApJ, 135, 736

Hester, J. J., et al. 1996, AJ, 111, 2349

Kun, M., Aoyama, H., Yoshikawa, N., Kawamura, A., Yonekura, Y., Onishi, T., & Fukui, Y. 2001, PASJ, 53, 1063

Lada, C. J. 1987, in IAU Symp. 115, Star Forming Regions, ed. J. Jugaku & M. Peimbert (Dordrecht: Reidel), 1

Lada, C. J. & Lada, E. A. 2003, ARA&A, 41, 57

Lee, H.-T., Chen, W. P., Zhang, Z., & Hu, J. 2005, ApJ, 624, 808 (Paper I)

Magakian, T. Y. 2003, A&A, 399, 141

McGroarty, F., Ray, T. P., & Bally, J. 2004, A&A, 415, 189

Odenwald, S., Fischer, J., Lockman, F. J., & Stemwedel, S. 1992, ApJ, 397, 174

Olano, C. A., Walmsley, C. M., & Wilson, T. L. 1994, A&A, 290, 235

Preibisch, T. & Zinnecker, H. 1999, AJ, 117, 2381

Schaerer, D. & de Koter, A. 1997, A&A, 322, 598

Schlegel, D. J., Finkbeiner, D. P., & Davis, M. 1998, ApJ, 500, 525

Spitzer, L. 1998, Physical Processes in the Interstellar Medium (New York: Wiley-Interscience)

Stanke, T., Smith, M. D., Gredel, R., & Szokoly, G. 2002, A&A, 393, 251

Thé, P. S., de Winter, D. & Pérez, M. R. 1994 A&AS, 104, 315

Waters, L. B. F. M., & Waelkens, C. 1998, ARA&A, 36, 233

White, G. J., Casali, M. M., & Eiroa, C. 1995, A&A, 298, 594

Wichmann, R. et al. 1996, A&A, 312, 439

Zacharias, N., Urban, S. E., Zacharias, M. I., Wycoff, G. L., Hall, D. M., Monet, D. G., & Rafferty, T. J. 2004, AJ, 127, 3043

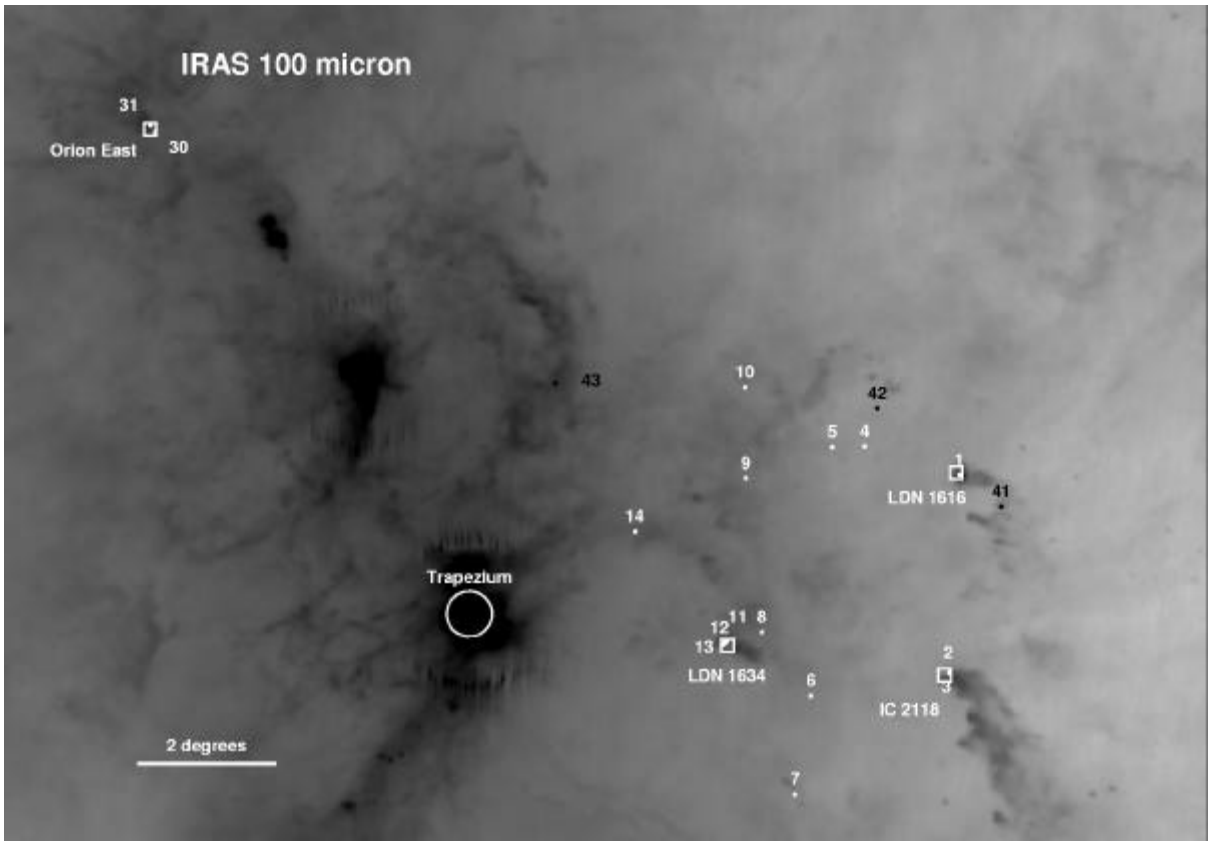

Fig. 1.— *IRAS* 100 μm image of the Orion region. The dots are the CTTSs (white) and the HAeBe stars (black) labeled with their serial numbers in Table 3 and 4. The boxes show the observed fields in Hα (Fig. 3). East is to the left and north to the top.

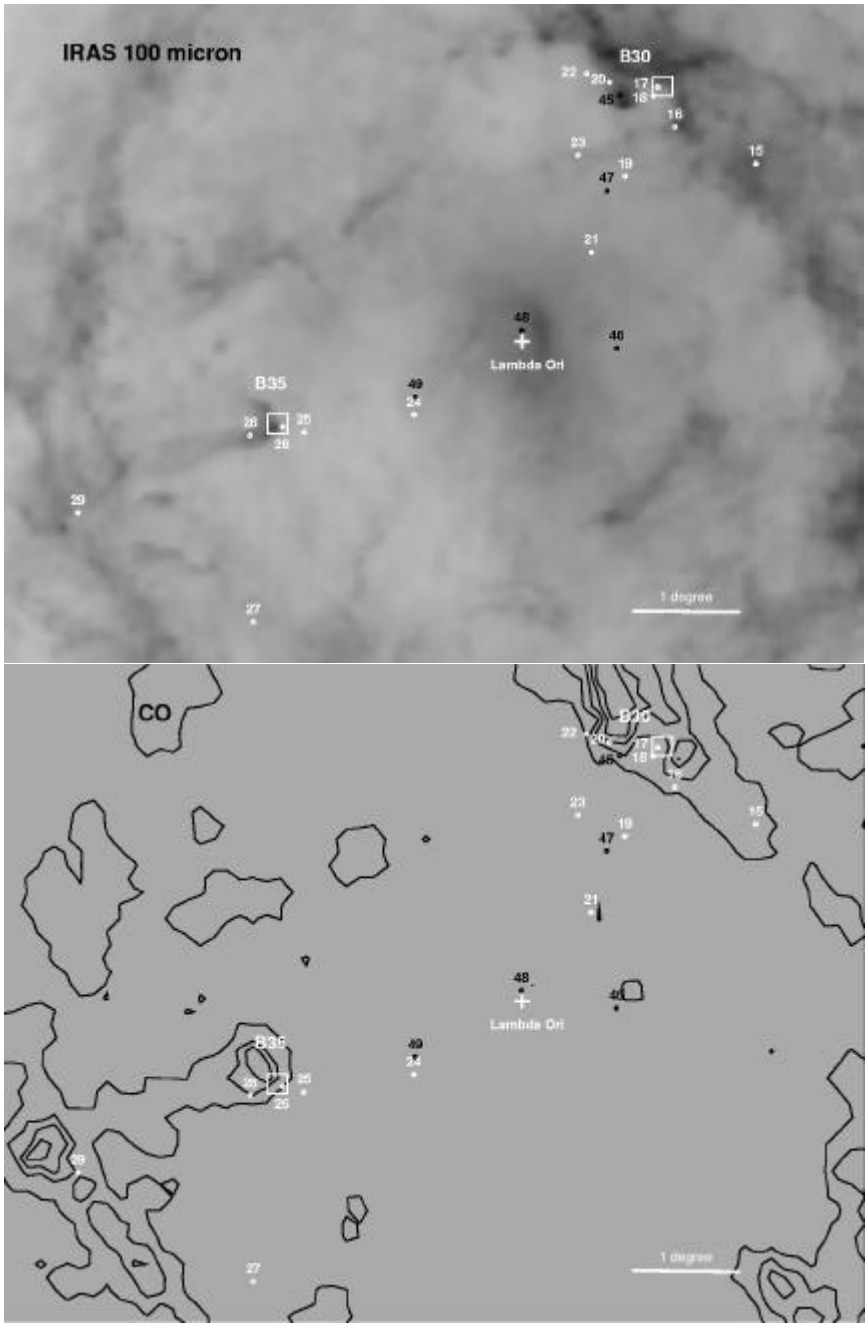

Fig. 2.— *IRAS* 100 μm and CO images of the λ Ori region. The symbols are the same as Figure 1. The distribution of PMS stars extends from λ Ori to the ends of B30 and B35. East is to the left and north to the top.

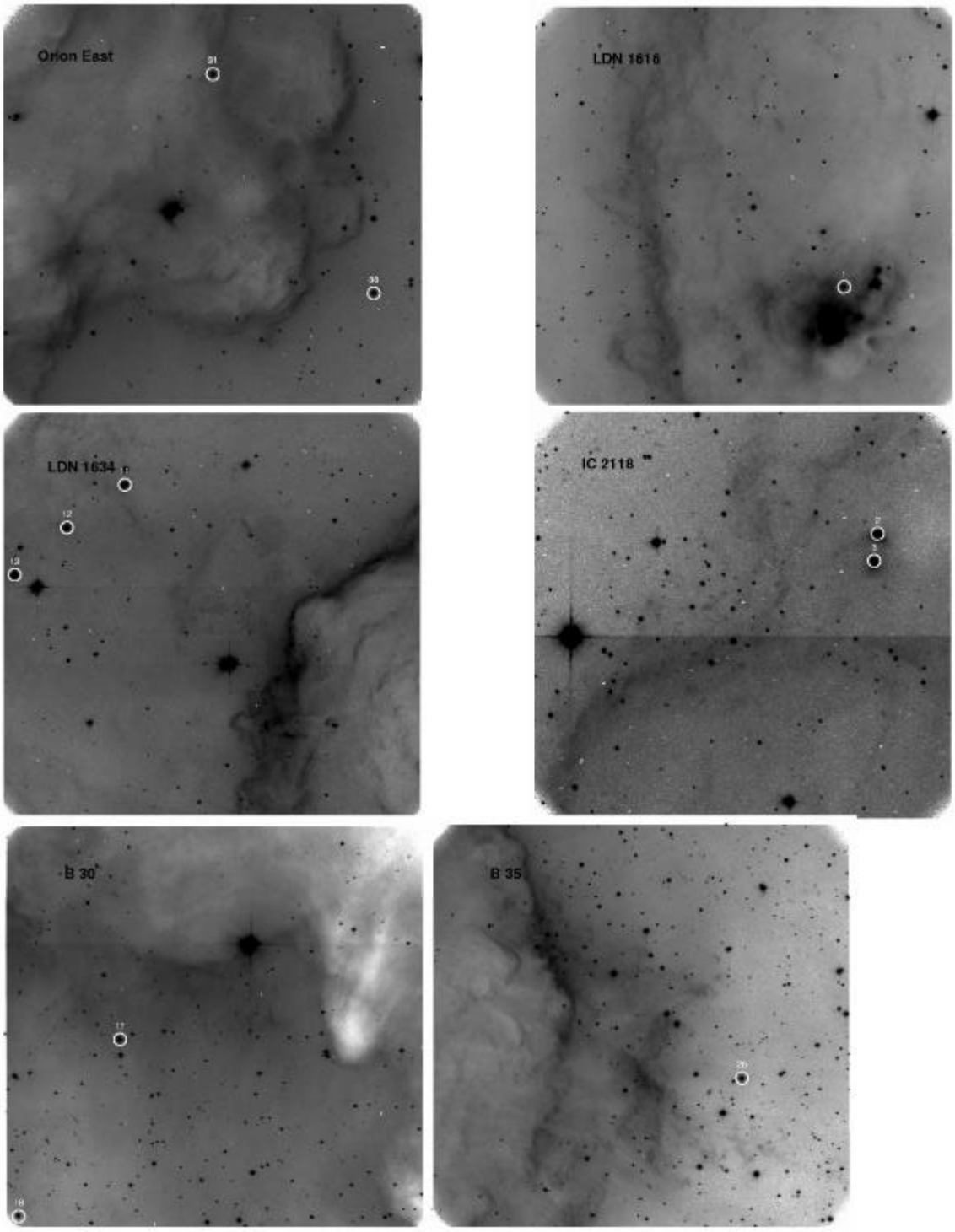

Fig. 3.— Hα images of the Ori OB1 BRCs. The stars in Table 3 are marked.

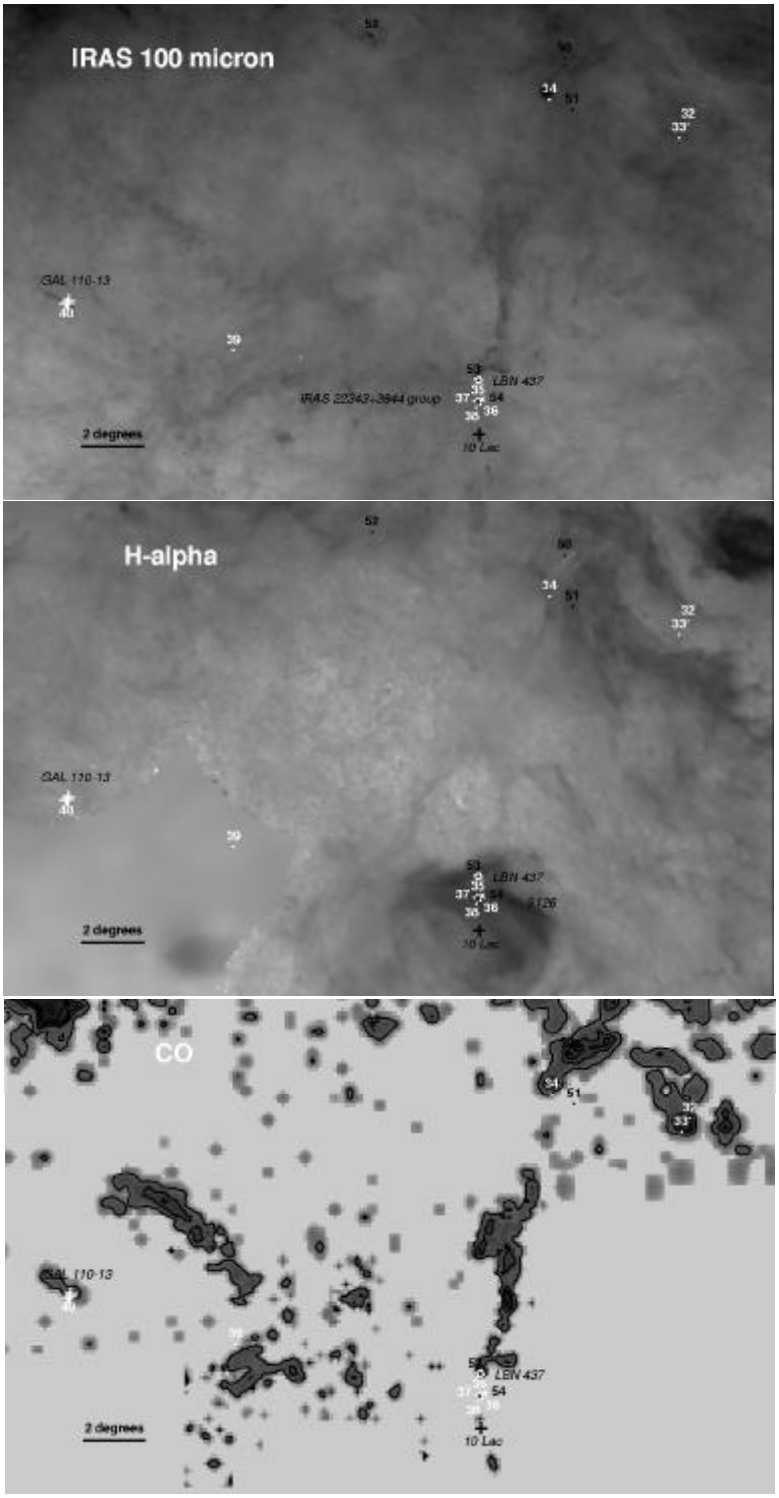

Fig. 4.— The *IRAS* 100 μm, Hα and CO images of the Lac OB1 association. The white pluses are the late B stars in GAL 110−13 and the cross in IRAS 22343+3944 is CTTS candidate, 2MASS J22354224+3959566, without spectra identification. The other symbols are the same as Figure 1. Galactic north is to the top.

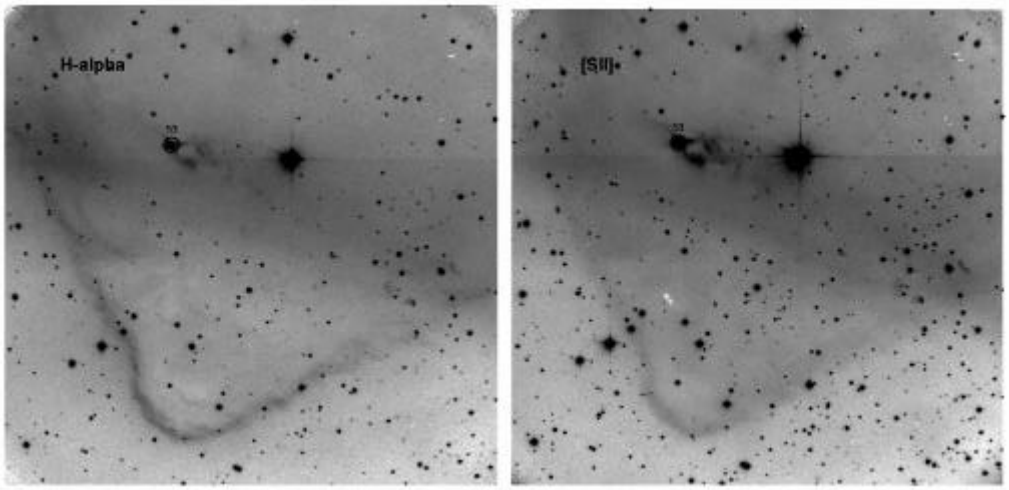

Fig. 5.— Hα and [SII] images of LBN 437. Star 53 is associated with HH 398.

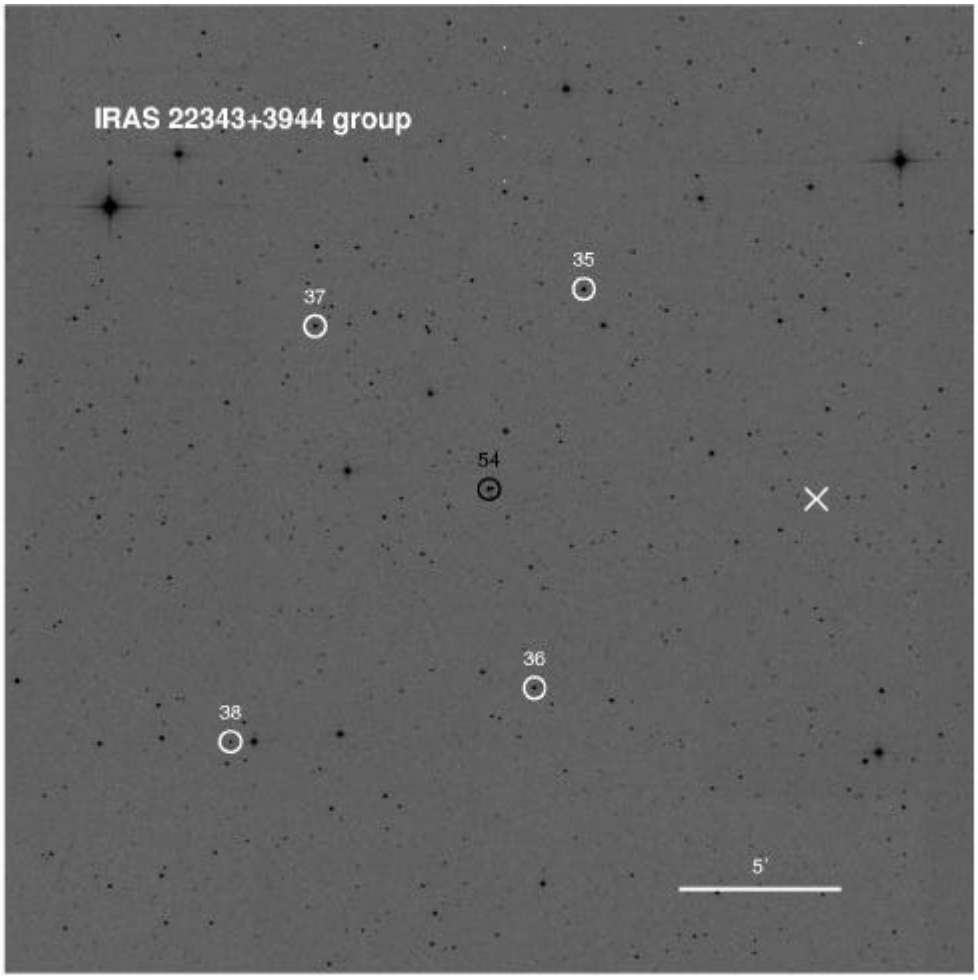

Fig. 6.— 2MASS Ks image of the IRAS 22343+3944 group. Stars in Table 3 (in white) and 4 (in black) are labled. The cross is the CTTS candidate, 2MASS J22354224+3959566. East is to the left and north to the top.

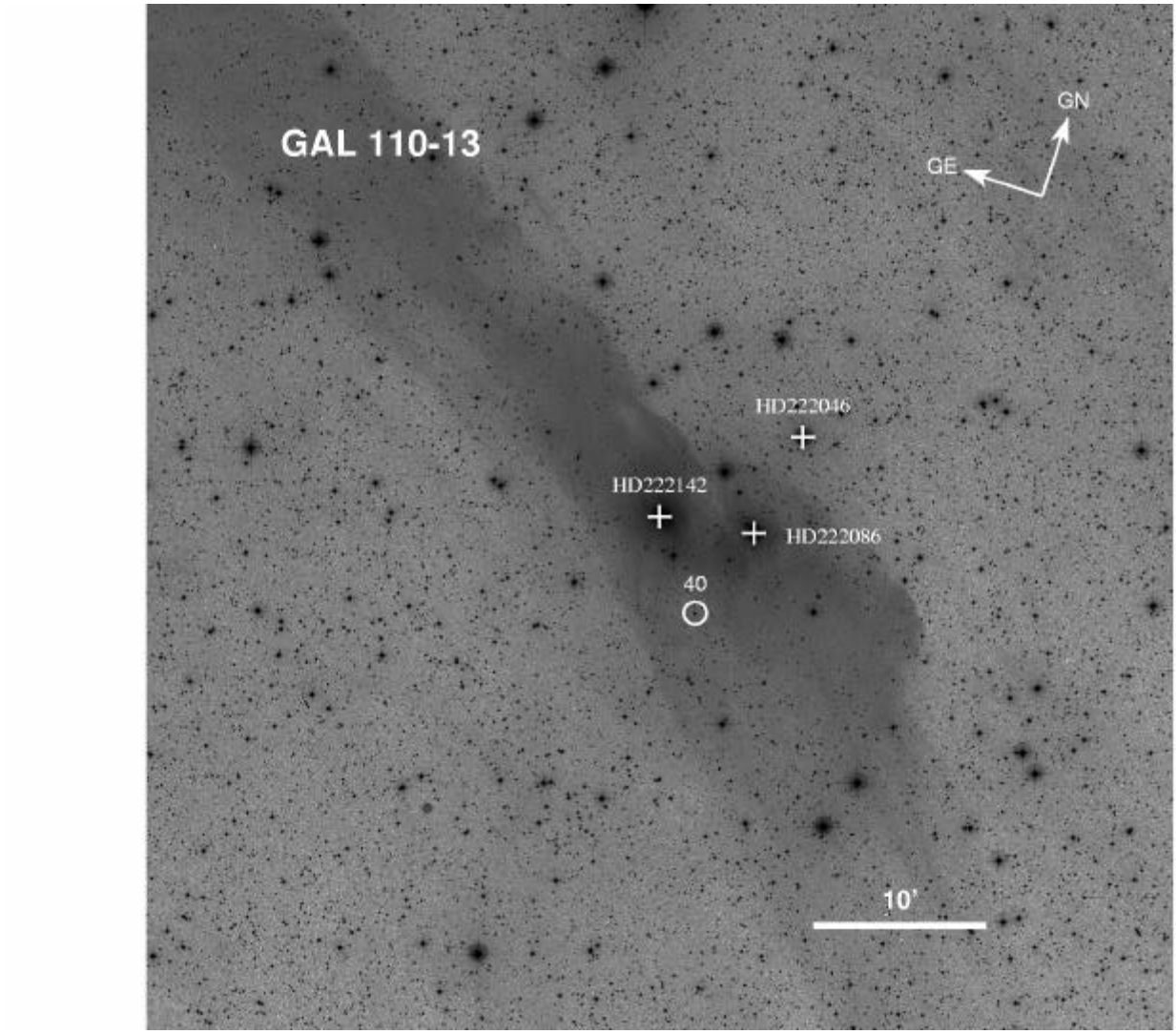

Fig. 7.— DSS blue image of the comet-shaped cloud GAL 110-13. Star 40 (CTTS) and three late B stars are marked. East is to the left and north to the top. Galactic north and east are also labled.

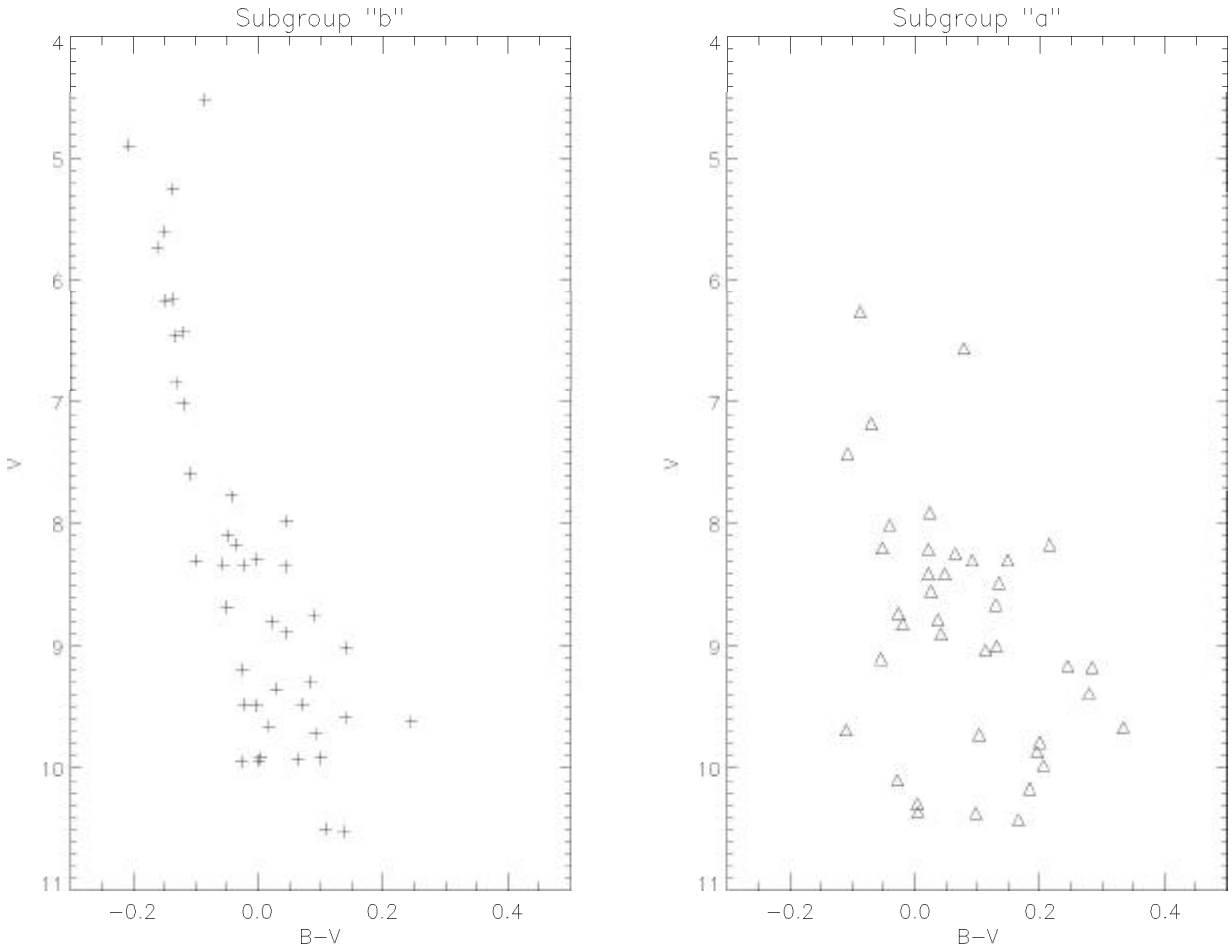

Fig. 8.— Color-magnitude diagrams of subgroups Lac OB1a and Lac OB1b. The stars in Lac OB1b (plus) gather to form a clear sequence (main sequence) in the diagram, whereas the stars in Lac OB1a (triangle) scatter much to the right of the sequence. It implies that Lac OB1a is younger than Lac OB1b.

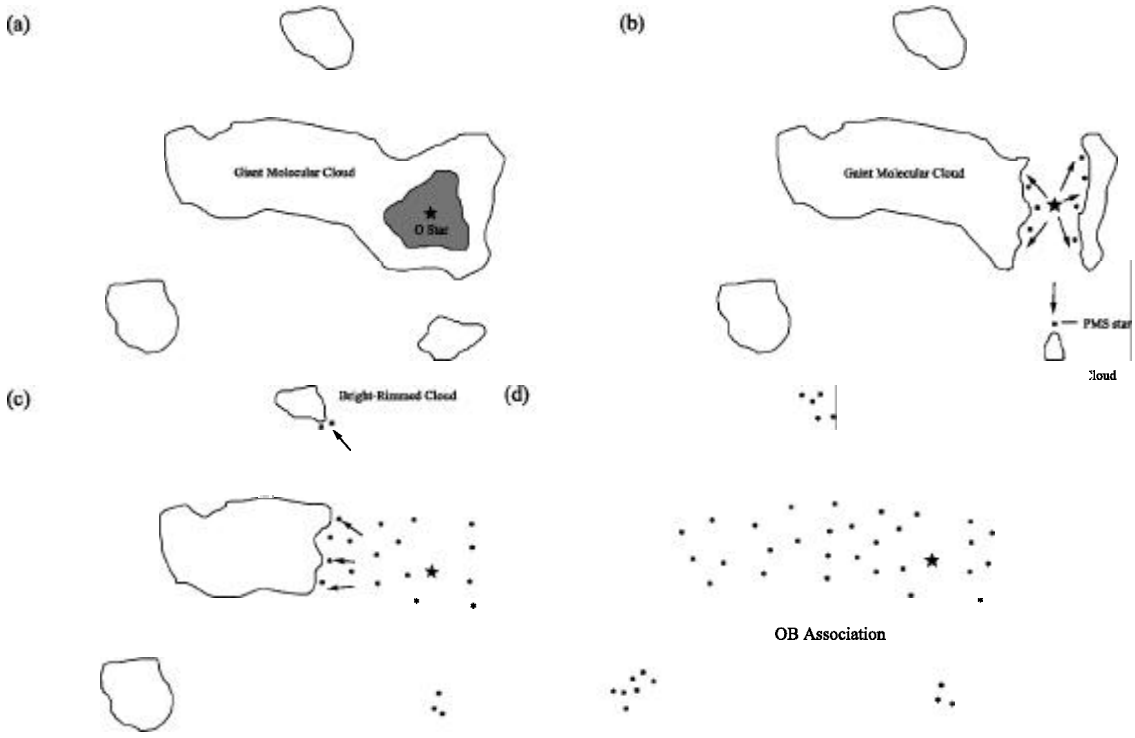

Fig. 9.— Formation of OB associations. O stars form inside a giant molecular cloud first (a) and then the expanding I-fronts will compress giant molecular clouds to form new stars, CTTSs and HAEBE stars. The I-fronts shape nearby clouds into BRCs and induce star formation (b, c). The star formation begins around O star and is spread out by expanding I-fronts. Eventually, tens of pc scale of OB associations would be formed (d).

Table 1. SELECTED REGIONS

region	RA or l	DEC or b
Lac OB1[a]	l 83° – 112°	b -3°.5 – -25°.7
Trapezium[b]	RA 5^h03^m – 5^h32^m	DEC -1°45′ – -8°10′
λ Ori[c]	RA 5^h23^m – 5^h52^m	DEC +6°40′ – +14°22′
Ori East	RA 5^h52^m – 5^h57^m	DEC +1°15′ – +2°15′
Control Field 1	l 192° – 260°	b +15° – +44°
Control Field 2	RA 20^h24^m – 21^h05^m	DEC +25°16′ – +32°55′

[a]Including BRC LBN 437 and comet-shaped cloud GAL 110−13

[b]Including BRCs, IC 2118, LDN 1616 and LDN 1634

[c]Including BRCs, B 30 and B 35

Table 2. Imaging Observations

Fields	RA	DEC	Filter	Total Exp. Time (s)
B30	05:29:51.4	+12:13:58	Hα	5400
B35	05:44:20.0	+09:10:40	Hα	5400
Ori East	05:53:58.6	+01:40:37	Hα	3600
LDN 1616	05:07:06.0	-03:17:54	Hα	7200
LDN 1634	05:20:16.0	-05:49:28	Hα	3600
IC 2118	05:07:44.0	-06:12:35	Hα	2400
LBN 437	22:34:31.0	+40:37:44	Hα	3600
LBN 437	22:34:31.0	+40:37:44	[S II]	7200

Table 3. CTTS and CTTS Candidates

Star	2MASS	Emission Line(s)	Li[a]	Obs.[b]	Remarks
1	J05065464-0320047	H, O, Ca, He	a	K	LkHa 333, associated with LDN 1616
2	J05073016-0610158	H, O, S, Fe, Ca, He	a	K	associated with IC 2118
3	J05073060-0610597	H, Ca?	a	K	associated with IC 2118
4	J05122053-0255523	H	a	K	V531 Ori
5	J05141328-0256411	H, O, Fe, Ca, He	n	K	Kiso A-0975 16
6	J05152683-0632010	H	a	K	Hα emission is week,could be a WTTS
7	J05162251-0756503	H, O, Ca, He	a	K	
8	J05181685-0537300	H, O, Fe, Ca, He	n	K	Kiso A-0975 43
9	J05191356-0324126	H, Ca, He	a	K	Kiso A-0975 45
10	J05191549-0204529	H, O, Ca	a	K	
11	J05201945-0545553	H, Ca, He	a	K	Kiso A-0975 52, IRAS 05178-0548, associated with LDN 1634
12	J05202573-0547063	H, O?, Fe, Ca, He	a	K	V534 Ori, associated with LDN 1634
13	J05203142-0548247	H, Ca, He	a	K	StHA 39, associated with LDN 1634
14	J05253979-0411020	H, Fe, Ca, He	n	K	Kiso A-0975 86
15	J05262158+1131339	H, O, Fe, Ca,	-	B	IRAS 05235+1129
16	J05292393+1151576	H, Ca, He	a	B, K	V649 Ori, associated with B 30
17	J05300203+1213357	H, Ca, He	a	B, K	GX Ori, IRAS 05272+1211, associated with B 30
18	J05301313+1208458	H, Ca	a	B, K	GY Ori, associated with B 30
19	J05311615+1125312	H, O	n	B, K	V449 Ori
20	J05315128+1216208	H, O, He	a	B, K	associated with B 30
21	J05323207+1044178	H, O?, Ca, He	-	B	
22	J05324305+1221083	H, O, Ca, He	a	B, K	V460 Ori, IRAS 05299+1219, associated with B 30

Table 3—Continued

Star	2MASS	Emission Line(s)	Li[a]	Obs.[b]	Remarks
23	J05330207+1137114	H, O?, Fe, Ca, He	-	B	
24	J05391268+0915522	H, O, Ca, He	-	B	
25	J05432091+0906071	H, O, Ca, He	a	B, K	V625 Ori, IRAS 05406+0904, associated with B 35
26	J05440899+0909147	H, O, Fe, Ca, He	a	B, K	QR Ori, IRAS 05413+0907, associated with B 35
27	J05451493+0721223	H	n	B, K	V661 Ori
28	J05452235+0904123		-	B	FU Ori, IRAS 05426+0903, associated with B 35
29	J05515035+0821066	H, Ca	a	B, K	
30	J05534090+0138140	H, O, S?, He	-	B	LkHA 334, IRAS F05510+0137, associated with Ori East
31	J05535869+0144094	H, Ca, He	-	B	LkHA 335, IRAS F05513+0143, associated with Ori East
32	J21370366+4321172	H, Fe, Ca, He	a	B, K	V1082 Cyg
33	J21395545+4313082	H, Ca	-	B	
34	J21535750+4659443	H	-	B	LkHA 256
35	J22361978+4006273	H, O, Ca	-	B	associated with IRAS 22343+3944 group
36	J22362779+3954066	H	-	B	associated with IRAS 22343+3944 group
37	J22370328+4005185	H, Ca?, He?	a	B, K	associated with IRAS 22343+3944 group
38	J22371683+3952260	H, O, Ca	-	B	associated with IRAS 22343+3944 group
39	J23104483+4508511	H	n	B, K	
40	J23373847+4824119	H	a	B, K	BM And

[a]a–absorbtion, n–no absorbtion, - –low spectral resolution in BAO

[b]B–BAO, K–KPNO

Table 4. Herbig Ae/Be Stars

Star	2MASS	Emission Line(s)	Sp. Type	Obs.[a]	Remarks
41	J05042998-0347142	H	A3e	K	UX Ori, IRAS 05020-0351, associated with LDN 1616
42	J05113654-0222484	H	A3e	K	
43	J05301868-0201575	H	A6e	K	HD 290543
44	J05305472+1421524	H	F2e	K	
45	J05312805+1209102	H, O	A2e	K	HK Ori, IRAS 05286+1207, associated with B 30
46	J05313515+0951553	H	B9e	K	IRAS 05288+0949
47	J05315724+1117414	H	A0e	B	HD 244604, IRAS 05291+1115
48	J05350960+1001515	H, O?	B9e	B	V1271 Ori, IRAS 05324+0959
49	J05390921+0925301	H	F7e	B, K	V506 Ori
50	J21462666+4744154	H, O	B9e	K	
51	J21514726+4615115	H	A9e	K	LR Cyg
52	J22154039+5215559	H	A2e	B	
53	J22344101+4040045	H, O, S	A2e	K	V375 Lac
54	J22363511+4000156	H, O	B8e	B	associated with IRAS 22343+3944 group

[a]B–BAO, K–KPNO

Table 5. Non-PMS Stars

Star	2MASS	Sp. Type	Obs.[a]	Remarks
1	J05285405-0606063	Me	K	Kiso A-0975 119, IRAS 05264-0608
2	J05232026+0934432	A0	B, K	TYC 704-1857-1
3	J05413010+1418225	C	K	BC 203
4	J05442880+0652019	M	B	
5	J05464207+0643469	C	B	IRAS 05440+0642
6	J05480851+0954012	Ce	B, K	V638 Ori, IRAS 05453+0953
7	J07323273+2647156	C	K	FBS 0729+269
8	J07475919+2052254	Ce	K	
9	J08231037-0153257	C	K	
10	J08292902+1046241	C	K	FBS 0826+109
11	J08423302+0621195	M	K	
12	J08541870-1200541	Ce	K	IRAS 08519-1149
13	J09111450-0922053	Me	K	VV Hya
14	J09333061-2216282	M	K	
15	J20245404+2609115	M	B	
16	J20291739+2617284	Me	B	IRAS 20271+2607
17	J20304177+2812340	M	B	DU Vul, IRAS 20285+2802
18	J20311267+2612270	M	B	
19	J20415136+2752525	M	B	IRAS 20397+2742
20	J20532040+2516196	C	B	
21	J20551307+3254065	M	B	
22	J20555284+2640515	M	B	UY Vul, IRAS 20537+2629
23	J21040556+2632111	M	B	V444 Vul, IRAS 21019+2620
24	J21244172+4437134	Ce	B	V1563 Cyg, IRAS 21228+4424
25	J21383182+4542469	Ce	K	V1568 Cyg, IRAS 21366+4529
26	J21595030+3313596	M	B	
27	J22024329+4216400	BL Lac	K	BL Lac
28	J22055958+3530057	M	B	XX Peg
29	J22070988+2828374	M	B	V392 Peg, IRAS F22048+2813
30	J22075421+4105113	M	B	V379 Lac, IRAS 22057+4050

Table 5—Continued

Star	2MASS	Sp. Type	Obs.[a]	Remarks
31	J22084406+4855248	M	B	V426 Lac, IRAS 22067+4840
32	J22121336+4646065	C	B	IRAS 22101+4631
33	J22135091+2447203	M	B	
34	J22213857+3335586	C	B	
35	J22261658+4221089	A0	B	
36	J22295650+4546539	Ce	B	V386 Lac
37	J22313443+4816005	C	K	V387 Lac, IRAS 22294+4800
38	J22314368+4748038	PN	K	PN G100.0-08.7, IRAS 22296+4732
39	J22451504+5051534	Ce	B	HL Lac, IRAS 22431+5036
40	J22491976+5154487	M	B	IRAS 22472+5138
41	J22514566+4921137	C	B	IRAS 22495+4905
42	J22521809+3413364	M	B	IRAS 22499+3357
43	J22592372+4811589	Me	K	
44	J23023314+4649483	M	B	NSV 14395, IRAS 23002+4633
45	J23113005+4702525	M	B	IRAS 23092+4646
46	J23175960+4645122	M	B	AO And, IRAS 23156+4628

[a]B–BAO, K–KPNO

Table 5. Proper Motions of Stars in GAL 110−13 and Lac OB1 Subgroup A and B

Star	Sp. type	pmRA (mas/yr)	pmDEC (mas/yr)	e_pmRA (mas/yr)	e_pmDEC (mas/yr)	Reference colhead
HD 222142	B9.5 V	0.3	-3.1	0.6	0.6	UCAC2
HD 222086	B9 V	0.5	-2.8	1.0	1.1	UCAC2
HD 222046	B8 Vp	0.4	-2.7	1.0	1.0	UCAC2
Star 40	Continuum	3.4	-7.8	2.7	2.6	UCAC2
Lac OB1a	-	-0.3	-3.7	-	-	Hipparcos
Lac OB1b	-	-0.5	-4.6	-	-	Hipparcos